J Vet Sci. 2020 Nov;21(6):e91
https://doi.org/10.4142/jvs.2020.21.e91
pISSN 1229-845X·eISSN 1976-555X

Journal of Veterinary Science

Original Article

Molecular and Cellular Biology

Check for updates

Anti-inflammatory effect of sulforaphane on LPS-stimulated RAW 264.7 cells and ob/ob mice

Sachithra S. Ranaweera, Chanuri Y. Dissanayake, Premkumar Natraj, Young Jae Lee, Chang-Hoon Han*

College of Veterinary Medicine, Jeju National University, Jeju 63243, Korea

OPEN ACCESS

Received: Sep 18, 2020
Revised: Oct 22, 2020
Accepted: Oct 28, 2020

***Corresponding author:**
Chang-Hoon Han
College of Veterinary Medicine, Jeju National University, 102 Jejudaehak-ro, Jeju 63243, Korea.
E-mail: chhan@jejunu.ac.kr

ORCID iDs
Sachithra S. Ranaweera
https://orcid.org/0000-0001-9589-3240
Chanuri Y. Dissanayake
https://orcid.org/0000-0002-1697-0293
Premkumar Natraj
https://orcid.org/0000-0003-2615-3809
Young Jae Lee
https://orcid.org/0000-0001-7892-5546
Chang-Hoon Han
https://orcid.org/0000-0002-0763-9590

Funding
This study was supported by the program of supporting Promising Small and Medium Industry (Grant No: C0518751) funded by the Korea Small and Medium Business Administration in 2017. The study was also supported by the 2019 scientific promotion program funded by Jeju National University.

ABSTRACT

Background: Sulforaphane (SFN) is an isothiocyanate compound present in cruciferous vegetables. Although the anti-inflammatory effects of SFN have been reported, the precise mechanism related to the inflammatory genes is poorly understood.
Objectives: This study examined the relationship between the anti-inflammatory effects of SFN and the differential gene expression pattern in SFN treated ob/ob mice.
Methods: Nitric oxide (NO) level was measured using a Griess assay. The inducible nitric oxide synthase (iNOS) and cyclooxygenase-2 (COX-2) expression levels were analyzed by Western blot analysis. Pro-inflammatory cytokines (tumor necrosis factor [TNF]-α, interleukin [IL]-1β, and IL-6) were measured by enzyme-linked immunosorbent assay (ELISA). RNA sequencing analysis was performed to evaluate the differential gene expression in the liver of ob/ob mice.
Results: The SFN treatment significantly attenuated the iNOS and COX-2 expression levels and inhibited NO, TNF-α, IL-1β, and IL-6 production in lipopolysaccharide (LPS)-stimulated RAW 264.7 cells. RNA sequencing analysis showed that the expression levels of 28 genes related to inflammation were up-regulated (> 2-fold), and six genes were down-regulated (< 0.6-fold) in the control ob/ob mice compared to normal mice. In contrast, the gene expression levels were restored to the normal level by SFN. The protein-protein interaction (PPI) network showed that chemokine ligand (Cxcl14, Ccl1, Ccl3, Ccl4, Ccl17) and chemokine receptor (Ccr3, Cxcr1, Ccr10) were located in close proximity and formed a "functional cluster" in the middle of the network.
Conclusions: The overall results suggest that SFN has a potent anti-inflammatory effect by normalizing the expression levels of the genes related to inflammation that were perturbed in ob/ob mice.

Keywords: Sulforaphane; anti-inflammatory activity; RNA sequencing analysis; differential gene expression; ob/ob mice

INTRODUCTION

Inflammation is the most commonly identified condition in the clinical field, which involves protecting the body from infection and tissue damage [1]. Macrophages are one of the

Conflict of Interest
The authors declare no conflicts of interest.

Author Contributions
Conceptualization: Han CH, Ranaweera SS; Data curation: Dissanayake CY; Formal analysis: Ranaweera SS; Funding acquisition: Han CH; Investigation: Ranaweera SS, Han CH; Methodology: Ranaweera SS; Project administration: Han CH; Resources: Han CH; Software: Premkumar N; Supervision: Han CH, Lee YJ; Validation: Han CH; Visualization: Ranaweera SS, Han CH; Writing - original draft: Ranaweera SS; Writing - review & editing: Premkumar N.

major groups of the immune system, which perform a critical role in response to injury and infection [2]. Nuclear factor-κB (NF-κB) is a key regulatory element in macrophages [3]. The activation of NF-κB is essential for the expression of nitric oxide (NO), inducible nitric oxide synthase (iNOS), cyclooxygenase-2 (COX-2), and pro-inflammatory cytokines, including tumor necrosis factor (TNF)-α, interleukin (IL)-6, and IL-1β [4]. Cytokines released from the inflammatory tissue disturb the metabolic functions of many organs, including the liver [5]. In particular, chronic inflammation is closely related to the progression of many metabolic diseases, including obesity and insulin resistance [6].

Obesity is associated with low-grade inflammation that causes oxidative stress, which leads to insulin resistance and non-alcoholic fatty liver disease (NAFLD) [7]. In the present study, ob/ob mice were selected as the appropriate *in vivo* model because they exhibit severe disturbances of the immune functions [8,9]. In particular, ob/ob mice have high levels of circulating endotoxin, which contributes to the development of inflammation by activating Toll-like receptor 4 (TLR4) signaling in the liver [8]. The inflammatory state of obesity is the augmented infiltration of T cells and macrophages into the metabolic tissues, including the liver [10]. In addition, ob/ob mice display hepatic lipid accumulation that induces inflammation, leading to NAFLD development [9]. Therefore, the liver of ob/ob mice was used to observe the effects of sulforaphane (SFN) on inflammatory gene expression.

SFN is an isothiocyanate present in cruciferous vegetables, such as cabbage, cauliflower, and broccoli [11]. Glucoraphanin (GRN), one of the main glucosinolates in cruciferous vegetables, is converted to SFN by the gut microbiota-derived myrosinase in both rodents and humans [12]. A previous study found that GRN ameliorates obesity-induced inflammation in high-fat diet-treated obese mice [13]. In addition, bioactivated GRN with myrosinase reduced pro-inflammatory signaling related to a spinal cord injury in an experimental mouse model [14]. The supplementation of GRN-rich broccoli sprout extract reduced inflammatory reactions in endothelial cells [15]. Furthermore, synthetic GRN exhibited anti-inflammatory activity by reducing TNF-α secretion in lipopolysaccharide (LPS)-stimulated THP-1 cells [16]. Because GRN has an anti-inflammatory effect *in vivo* and *in vitro*, the present study used it as a control to compare the anti-inflammatory effect with SFN on both RAW 264.7 cells and ob/ob mice. SFN shows high chemical reactivity because of the electrophilicity of its isothiocyanate group [17]. Previous studies reported that SFN prevents oxidative stress-induced inflammation [18]. Furthermore, the SFN treatment prevented nod-like receptor protein 3 (NLRP3) inflammasome-induced NAFLD in obese mice [19]. Despite the anti-inflammatory and antioxidant effects of SFN, its exact mechanism related to the inflammatory genes is not completely understood.

The present study examined the anti-inflammatory activity of SFN on LPS-stimulated RAW 264.7 cells and ob/ob mice. The effects of SFN on the expression levels of pro-inflammatory mediators, such as NO, COX-2, iNOS, TNF-α, IL-6, and IL-1β, were analyzed in LPS-stimulated RAW 264.7 cells. In addition, the effects of SFN on obesity-related inflammation was identified from the expression levels of genes related to inflammation in ob/ob mouse livers.

MATERIALS AND METHODS

DPPH radical scavenging activity

The antioxidant activity of the SFN was evaluated using stable free radical 2,2-diphenyl-1-picrylhydrazyl (DPPH) according to a slight modification of a previously described method [20]. Various concentrations of SFN (Sigma, USA) and GRN (Cayman Chemicals, USA) were diluted in dimethyl sulfoxide (DMSO) (Sigma) and incubated with ethanolic 0.1 mM DPPH (Sigma) at 37°C for 30 min. The absorbance was measured at 517 nm using a UV spectrophotometer (Mecasys, Korea). The blanks were prepared by replacing the sample volumes with DMSO. The results were calculated as percentages of the control (100%), and the concentration of extracts required to decrease the initial DPPH concentration by 50% was expressed as the IC_{50} value. The radical scavenging ability (%) of the samples was calculated as % inhibition = $[(A_{Blank} - A_{sample})/A_{Blank}] \times 100$, where A_{Blank} = absorbance of the DPPH without the sample and A_{sample} = absorbance of the SFN or GRN. The antioxidant activity of the SFN is expressed as the ascorbic acid (AA) equivalent antioxidant capacity (AEAC) as AA/100 g dry weight (DW) using the equation, AEAC = $IC_{50\ (Ascorbic\ acid)}/IC_{50\ (Sample)} \times 10^5$.

Measurement of NO production

The murine macrophage RAW 264.7 cell line (KCLB 40071) was purchased from the Korean cell line bank (KCLB, Korea). The cells were cultured in Dulbecco's modified Eagle's medium (DMEM), containing 10% fetal bovine serum (FBS), 1% penicillin-streptomycin (Gibco, Thermo Fisher Scientific, USA), and kept at 37°C in a humidified atmosphere containing 5% CO_2. After reaching 70–80% confluence, the cells were sub-cultured within two-day intervals. For the experiment, the cells were cultured in 96 well plates. After 24 h incubation, the cells were pretreated with SFN (2.5 and 5 μM) and GRN (5 μM) for 1 h, and then stimulated with LPS (Escherichia coli 0111:B4; Sigma-Aldrich, USA) for 24 h. The concentration of SFN was determined according to a previous study [21], and the same concentration (5 μM) of GRN was used to compare its activity with SFN. The level of NO production by LPS-stimulated RAW 264.7 macrophage cells was determined by measuring the nitrite level in the culture media using Griess reagent (Promega, USA). Briefly, the 50 μL of culture media from each well was mixed with 50 μL of N-(1-naphthyl)ethylenediamine dihydrochloride (NED) and 50 μL of a sulfanilamide solution. After incubating the mixture for 10 min at room temperature, the absorbance was read at 550 nm in an enzyme-linked immunosorbent assay (ELISA) microplate reader (TECAN, Austria).

ELISA

RAW 264.7 macrophage cells were cultured in 96 well plates (1×10^5 cells/well) in DMEM, 10% FBS, and 1% penicillin-streptomycin. After 24 h of incubation, the cells were pretreated with SFN and GRN and then stimulated with LPS for 24 h. The concentrations of TNF-α, IL-6, and IL-β in the culture media were measured using commercially available ELISA kits (Koma Biotech, Korea) according to the manufacture instructions.

Measurement of COX-2 and iNOS protein expression

RAW 264.7 macrophage cells were cultured in six-well plates (1×10^6 cells/well) in DMEM, 10% FBS, and 1% penicillin-streptomycin. After 24 h incubation, the cells were pretreated with SFN and GRN for 1 h and then stimulated with LPS for 24 h. The expression levels of the COX-2 and iNOS proteins were observed by Western blot analysis. The cells were lysed with RIPA buffer containing a protease inhibitor mixture. The supernatant was separated, and the protein concentrations were evaluated using the Bradford assay (Bio-Rad Laboratories,

USA). The equal amount of protein was mixed with 20% of loading buffer and separated by Tris-Glycine-Polyacrylamide, non-sodium dodecyl sulfate precast gel (10%, Koma Biotech) and subjected to Western blot with COX-2 (Sigma), iNOS (Sigma), and β-actin (Thermofisher, USA) antibodies. A Chemi-luminescence Bioimaging Instrument (NeoScience Co., Korea) was used to detect the proteins of interest.

Animals experiments

Male ob/ob mice (6 weeks old) were purchased from Japan SLC Inc. (Japan). The mouse strain was originated from Jackson Laboratory (USA) [22], and was developed to C57BL/6JHamSlc-ob in Japan SLC Inc. (Japan). Male C57BL/6 mice (6 weeks old) supplied by Orient Bio (Korea) were used as the non-obesity control group. The mice were housed at a controlled temperature (24°C ± 1°C) and 50-55% humidity with a 12 h light/12 h dark cycle. All experiments were carried out according to the National Institute of Health Guide for the Care and Use of Laboratory Animals and were approved by the Institutional Animal Care and Use Committee of Jeju National University (ACUCC; approval No. 2018-0051).

Sample treatment

The ob/ob mice were allocated randomly into three groups (n = 5): control ob/ob group and 2 sample-treated groups were orally administrated SFN (0.5 mg/kg), and GRN (2.5 mg/kg) every day in their drinking water assuming that each mouse drinks 20 mL of water per day. The concentrations of SFN and GRN were selected based on previous studies [23]. The samples were diluted with distilled water, and the mice were given access to water and food ad libitum. The samples were replaced with freshly prepared solutions every day to compensate for the degradative loss of the active compounds. After 6 weeks of sample treatment, the mice were fasted overnight and sacrificed. The liver tissues were collected and stored at −80°C for further experiments.

Measurement of triglyceride (TG) content in liver tissues of ob/ob mice

Hepatic TG contents were quantified using a commercially available TG colorimetric assay kit (BioAssay Systems, USA). Briefly, the liver tissues were homogenized with 5% Triton X-100 (Bio-Rad Laboratories) and centrifuged at 13,000 ×g for 10 min to separate the fat layer. The TG and protein contents of the diluted supernatants were analyzed according to the manufacturer's instructions. The protein concentration of each sample was measured using a Bio-Rad DC protein assay (Bio-Rad Laboratories). The TG contents were normalized to the respective protein concentration, employing bovine serum albumin (Sigma) as the calibration standard.

Total RNA isolation, library preparation, sequencing, and data analysis

The total RNA was purified from liver tissues using an Easy-blue RNA extraction kit (iNtRON Biotechnology, Korea) according to the manufacturer's protocol. The RNA quality and quantity were analyzed on an Agilent 2100 bioanalyzer using the RNA 6000 Nano Chip (Agilent Technologies, Netherlands) and ND-2000 Spectrophotometer (Thermofisher), respectively. The control and test RNA libraries were constructed using Ouantseq 3′ mRNA-Seq Library Prep Kit (Lexogen, Austria). Briefly, 500 ng of the total RNA was prepared, and an oligo-dT primer containing an Illumina-compatible sequence at its 5′ end was hybridized to the RNA. Reverse transcription was then performed. Following degradation of the RNA template, complementary strand synthesis was initiated by a random primer containing an Illumina-compatible linker sequence at its 5′ end. Magnetic beads were used to eliminate all

the reaction components. The library was amplified to add the complete adaptor sequences required for cluster generation. The constructed library was purified from the polymerase chain reaction mixture. High-throughput sequencing was performed as single-end 75 sequencings using Illumina NextSeq 500 (Illumina, USA). The QuantSeq 3′ mRNA-Seq reads were aligned using Bowtie2 version 2.1.0. The Bowtie2 indices were either generated from representative transcript sequences or the genome assembly sequence to align with the transcriptome and genome. The alignments were used to assemble transcripts, estimating their abundances, and detecting differential expression of genes. The differentially expressed genes were determined based on the counts from unique and multiple alignments using R version 3.2.2 and Bioconductor version 3.0. The Read count (RT) data were analyzed based on the Quantile normalization method using the Genowiz™ version 4.0.5.6 (Ocimum Biosolutions, India). The PPI network was analyzed using the STRING application tool. Cytoscape (version 2.7), a bioinformatics platform at the Institute of System Biology, USA, was used to construct the network diagrams. Gene classification was performed using the Medline database (National Center for Biotechnology Information, USA).

Statistical analysis

Values are expressed as the means ± SE of three independent experiments. The data were statistically analyzed using IBM SPSS Statistics (Ver.17.0; USA). The statistical differences between the groups were observed with one-way analysis of variance (ANOVA) followed by a Turkey's test. The $p < 0.05$, $p < 0.005$, and $p < 0.0005$ indicate statistically significant differences from the control group.

RESULTS

DPPH radical scavenging activity of SFN

The antioxidant activity of the SFN was evaluated based on the DPPH assay. According to the results, the DPPH free radical scavenging activity was increased significantly ($p < 0.0005$) by SFN. In contrast, GRN did not exhibit any free radical scavenging activity compared to the control (**Fig. 1**). SFN showed up to 58% radical scavenging activity with 500 μg/mL SFN. The calculated IC_{50} values of SFN and GRN were 405.79 ± 14.6 and 4163.5 ± 167 μg/mL, respectively (**Table 1**). In addition, the AEAC of SFN and GRN was 2,557.97 ± 89.08 and

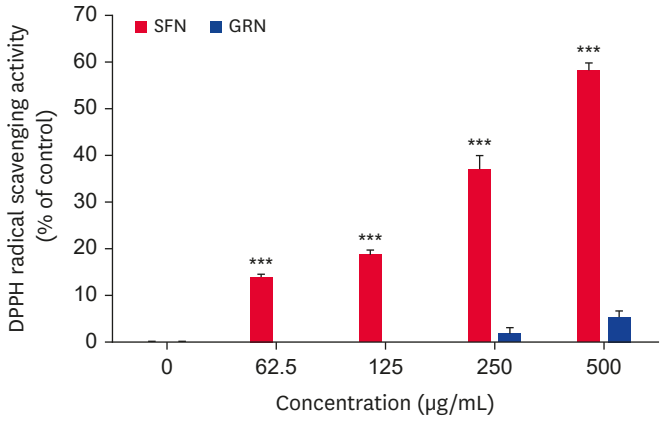

Fig. 1. DPPH radical scavenging activity of SFN. The results are the means of ± SE for three independent experiments.
DPPH, 2,2-diphenyl-1-picrylhydrazyl; SFN, sulforaphane; GRN, glucoraphanin.
***$p < 0.0005$ compared to the control.

https://doi.org/10.4142/jvs.2020.21.e91

Table 1. Antioxidant activity of samples expressed as IC_{50} and AEAC values

Sample	Antioxidant activity	
	IC_{50} values (μg/mL)	AEAC value
SFN	405.79 ± 14.6	2,557.97 ± 89.08
GRN	4,163.5 ± 167	249.309 ± 8.22
AA	10.38 ± 0.12	-

Values represent as mean ± SE.
IC_{50}, the concentration at which 50% of free radical scavenged; AEAC, AA equivalent antioxidant capacity expressed as AA/100 g dry weight; AA, ascorbic acid; SFN, sulforaphane; GRN, glucoraphanin.

249.309 ± 8.22 mg AA/100g, respectively (**Table 1**). These results indicate that SFN showed antioxidant potential through the free radical scavenging.

Inhibition of LPS-stimulated NO production by SFN

To examine the effects of SFN on LPS-stimulated NO production, the amount of NO released from the cells was determined using a Griess assay. In addition, the cell morphology was observed to ensure the experiments were performed under the right conditions. As shown in **Fig. 2A**, the morphologies of the RAW 264.7 cells were not changed after treating the SFN and GRN with LPS compared to the control cells. The results suggested that both SFN and GRN used in this study do not alter the RAW 264.7 cell morphology. Based on the Griess assay results, NO production was increased significantly after the LPS treatment in RAW 264.7 cells compared to the normal cells (**Fig. 2B**). The treatment of SFN inhibited LPS-stimulated NO

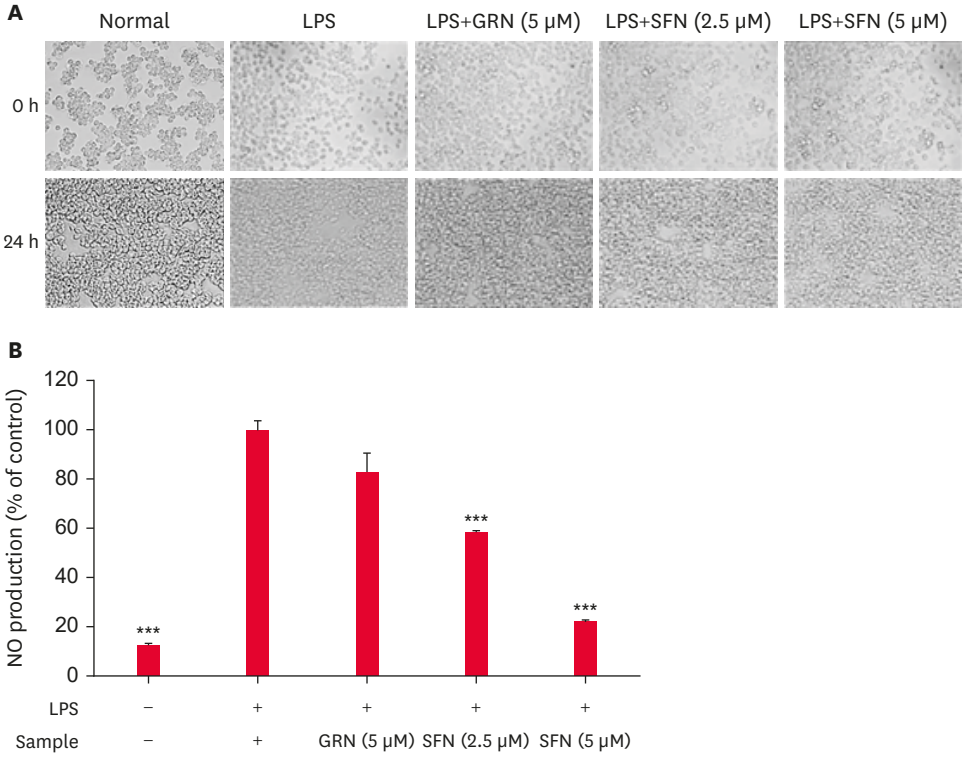

Fig. 2. Cell morphology and NO production in LPS-stimulated RAW 264.7 cells. Phase-contrast microscopy (20×) showing the morphology of RAW 264.7 cells before and after incubation with samples for 24 h (A). NO production by LPS-stimulated RAW 264.7 cells treated with or without SFN and GRN (B). All data are expressed as the mean ± SE.
NO, nitric oxide; LPS, lipopolysaccharide; SFN, sulforaphane; GRN, glucoraphanin.
***$p < 0.0001$ compared to the control.

https://doi.org/10.4142/jvs.2020.21.e91

production in a concentration-dependent manner, whereas the GRN treatment showed no significant change in NO production. The inhibition level of LPS-stimulated NO production was decreased significantly to 42% and 78% at 2.5 μM and 5 μM of SFN compared to the LPS-treated control cells. The result confirmed that SFN inhibited NO production in LPS-stimulated RAW 264.7 cells.

Effects of SFN on COX-2 and iNOS expression in LPS-stimulated RAW 264.7 cells

The inhibitory effect of SFN on the expression levels of the COX-2 and iNOS proteins in LPS-stimulated RAW 264.7 cells were investigated by Western blot analysis. The cells treated with SFN showed significant decreases in the levels of COX-2 and iNOS compared to the LPS treated control cells. In contrast, the GRN-treated cells did not significantly affect COX-2 or iNOS expression (**Fig. 3**) compared to the control cells. The results suggest that SFN regulates inflammation by inhibiting iNOS and COX-2 in LPS-stimulated RAW 264.7 cells.

Inhibitory effects of SFN on TNF-α, IL-6, and IL-1β production

The effects of SFN on the LPS-stimulated pro-inflammatory cytokines, TNF-α, IL-6, and IL-1β production were investigated in RAW 264.7 cells. Treatment of SFN showed significant inhibition ($p < 0.05$) of TNF-α, IL-6, and IL-1β production. In contrast, GRN did not significantly affect the production of those cytokines in LPS-stimulated RAW cells (**Fig. 4**). SFN inhibited the LPS-stimulated TNF-α, IL-6, and IL-1β production by 32%, 31%, 53%, respectively, at 5 μM compared to the control. These results confirmed that SFN inhibits the pro-inflammatory cytokines in LPS-stimulated RAW 264.7 cells.

Effect of SFN on TG accumulation in ob/ob mice liver

Because excessive TG accumulation is a key factor in liver inflammation, the present study showed the hepatic TG content in ob/ob mice. Based on the results, the ob/ob mouse livers showed higher levels of TG accumulation than the normal mouse liver (**Fig. 5**). In particular,

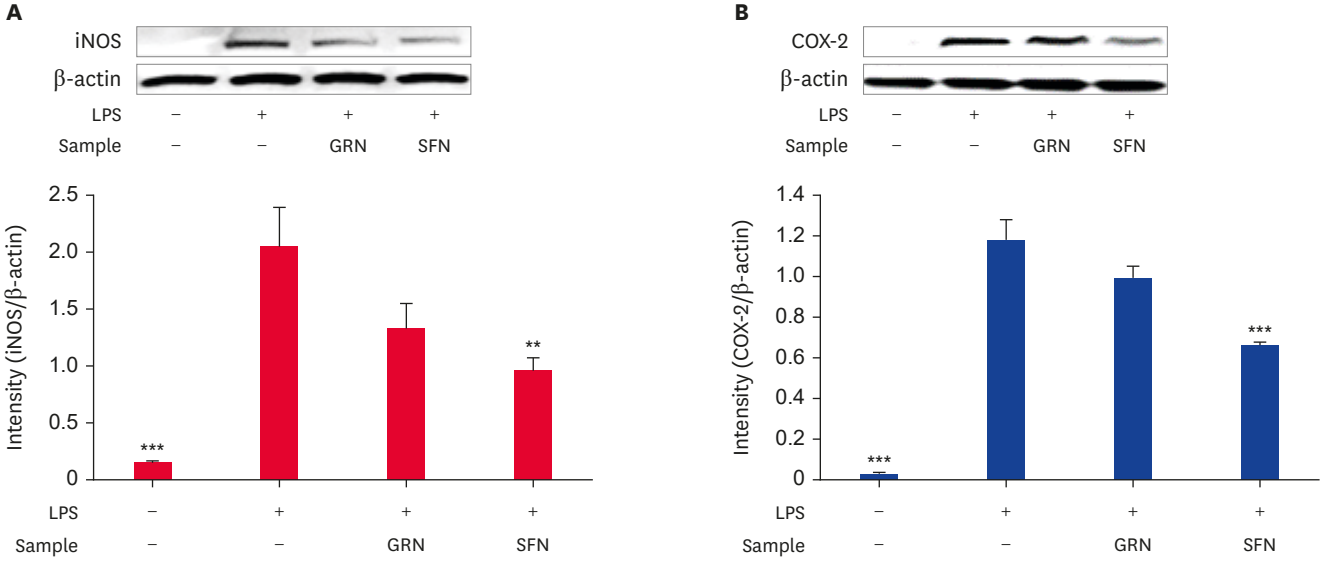

Fig. 3. Effects of SFN on iNOS and COX-2 expressions in LPS-stimulated RAW 264.7 cells. Cells were incubated with or without samples (SFN 5 μM, GRN 5 μM) and LPS for 24 h. The iNOS and COX-2 protein expression levels were determined by Western blotting, and the relative levels of iNOS (A) and COX-2 (B) proteins were normalized to β-actin. All data are expressed as mean ± SE.
SFN, sulforaphane; iNOS, inducible nitric oxide synthase; LPS, lipopolysaccharide; GRN, glucoraphanin; COX-2, cyclooxygenase-2.
$^{**}p < 0.005$, $^{***}p < 0.0005$ compared to the control.

https://doi.org/10.4142/jvs.2020.21.e91

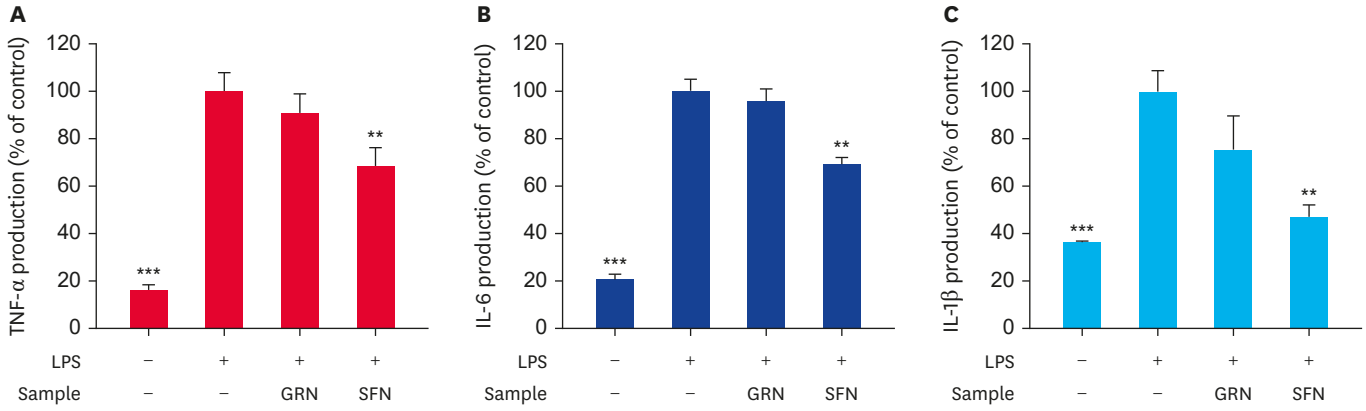

Fig. 4. Effects of SFN on the productions of pro-inflammatory cytokines in LPS-stimulated RAW 264.7 macrophage cells. Cells were incubated with or without samples (SFN 5 μM, GRN 5 μM) and LPS for 24 h. The levels of IL-1β, IL-6, and TNF-α released by LPS-stimulated RAW 264.7 cells into the culture supernatants were measured by ELISA assay kit. Production of TNF-α (A), production of IL-6 (B), and production of IL-1β (C) by LPS-stimulated RAW 264.7 cells. All data are expressed as mean ± SE.
SFN, sulforaphane; LPS, lipopolysaccharide; GRN, glucoraphanin; IL, interleukin; TNF, tumor necrosis factor; ELISA, enzyme-linked immunosorbent assay.
$^{**}p < 0.005$, $^{***}p < 0.0005$ compared to the control.

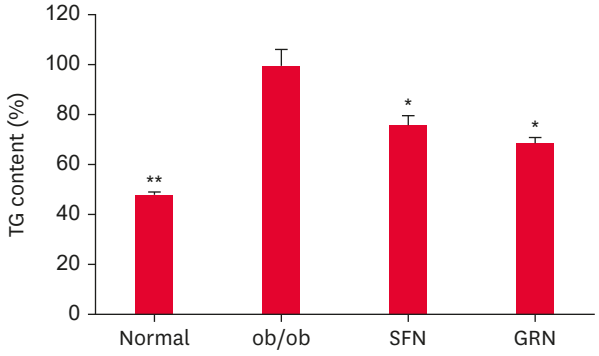

Fig. 5. Effect of SFN on hepatic TG content in ob/ob mice. Mice on the indicated diet for 6 weeks were (n = 4/group) sacrificed. Liver tissue lysate was subjected to TG analysis. All data are expressed as mean ± SE.
SFN, sulforaphane; TG, triglyceride; GRN, glucoraphanin.
$^{*}p < 0.05$, $^{**}p < 0.05$ compared with control ob/ob group.

the ob/ob mice treated with both SFN and GRN showed 24% and 32% lower hepatic TG contents, respectively, compared to the control ob/ob mice. These results suggest that SFN reduces hepatic TG accumulation, which might normalize liver inflammation in ob/ob mice.

Differential gene expression analysis of ob/ob mice liver

RNA sequencing analysis was performed to observe the effects of SFN on the expression levels of the genes related to inflammation in ob/ob mice. The functional annotation of the genes was evaluated by Gene Ontology (GO) analysis. As shown in **Fig. 6**, a large portion of the genes related to inflammation was up- or down-regulated in the SFN and GRN-treated ob/ob mice compared to normal mice. The up-regulated (> 2-fold) 28 genes, including Ccl1, Ccl4, Cxcr1, Ccr3, and Ifng, and 6 down-regulated (lower than 0.6-fold) genes, including Fn1, Itgb2l, Pik3cd, and Adora2a, were normalized to the control level by the SFN treatment (**Tables 2** and **3**). The PPI network was constructed using the STRING analysis to understand the relationship between normalized genes by SFN. The PPI network was visualized as nodes (genes) and edges (interactions between the genes), as shown in **Fig. 7**. Among the proteins related to inflammation, the chemokine ligands (Ccl1, Ccl4, Ccl3, and Ccl17) and chemokine receptors (Cxcr1, Ccr3, and Ccr10) were closely associated and formed a large "functional

https://doi.org/10.4142/jvs.2020.21.e91

cluster" in the middle of the network (**Fig. 7**). The present results confirmed that SFN restored the expression levels of the genes related to inflammation to the normal level, which were up or down-regulated in ob/ob mice.

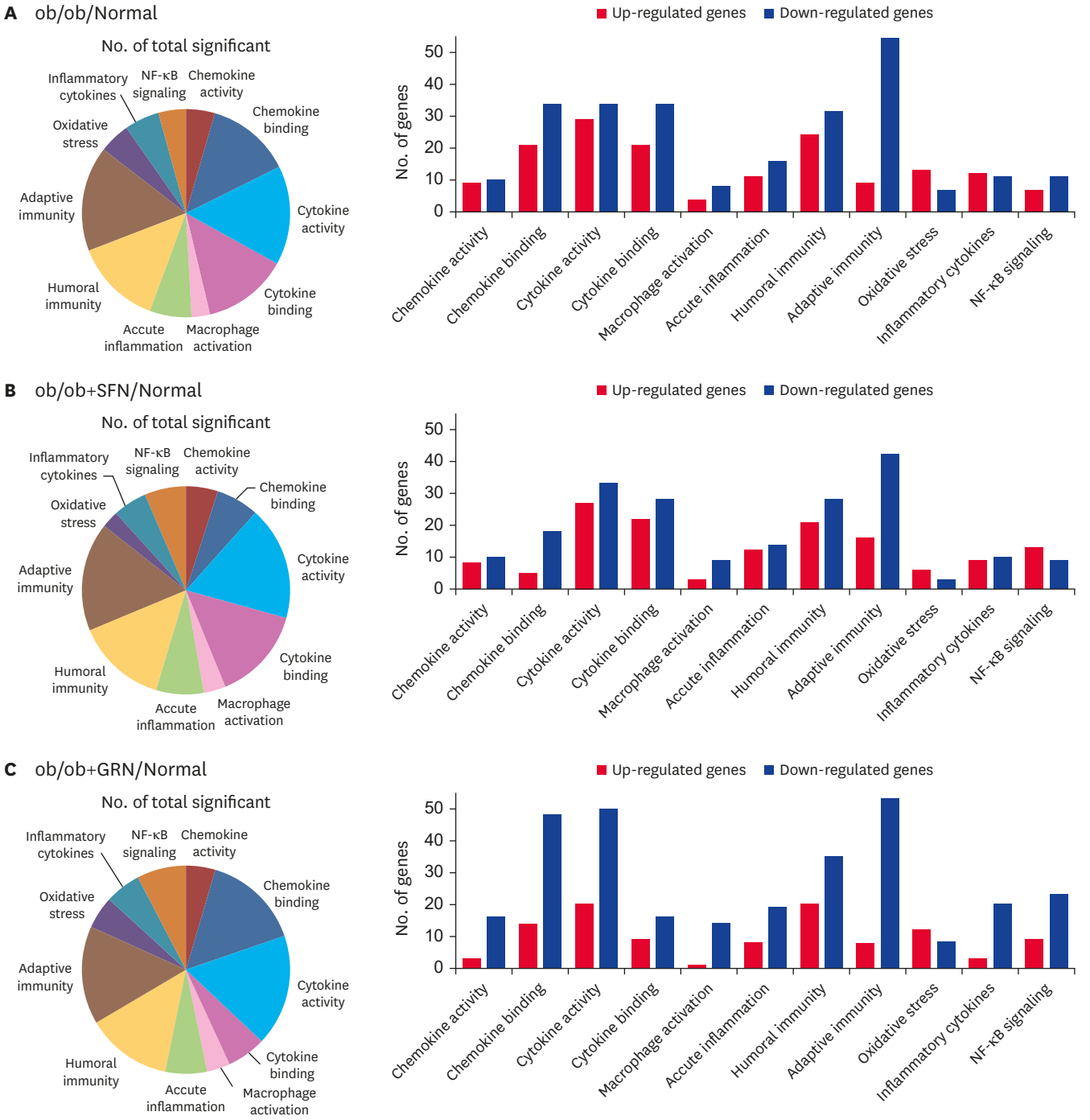

Fig. 6. Effect of SFN on differential gene expression in ob/ob mice liver. GO analysis of control ob/ob mice compared to the normal mice (A); SFN treated ob/ob mice compared to the normal mice (B), GRN-treated ob/ob mice compared to the normal mice (C) (The pie chart indicates functional categorization of the differentially expressed genes in ob/ob mice liver, and the bar graph represents the number of genes up and down-regulated).
SFN, sulforaphane; GO, Gene Ontology; GRN, glucoraphanin; NF, nuclear factor.

https://doi.org/10.4142/jvs.2020.21.e91

Table 2. Up-regulated inflammatory genes in the liver of ob/ob mice and normalized by SFN

Gene symbol	ob/ob/normal	SFN/normal	GRN/normal	Gene name
Gpx2	16.245	0.951	0.954	Glutathione peroxidase 2
Alox5	10.686	0.944	0.947	Arachidonate 5-lipoxygenase
Cst7	7.909	1.750	1.889	Cystatin F (leukocystatin)
Fut7	7.358	0.968	0.969	Fucosyltransferase 7
Zfr2	7.220	0.955	0.958	Zinc finger RNA binding protein 2
Nqo1	6.633	2.785	3.459	NAD(P)H dehydrogenase, quinone 1
Dcst1	6.488	0.973	1.956	DC-STAMP domain containing 1
Eomes	4.736	0.987	0.988	Eomesodermin
Ccl17	4.091	0.896	0.902	Chemokine (C-C motif) ligand 17
Ifng	3.785	0.987	0.988	Interferon gamma
Pdgfb	3.729	2.094	1.991	PDGF, B polypeptide
Ccl1	3.728	1.022	0.980	Chemokine (C-C motif) ligand 1
Trem1	3.572	1.592	0.956	Triggering receptor in myeloid
Cxcl14	3.231	1.448	1.255	Chemokine (C-X-C motif) ligand 14
Cxcr1	3.231	1.114	1.031	Chemokine (C-X-C motif) receptor 1
Lgals3	3.008	1.061	0.811	Lectin, galactose binding, soluble 3
Tnfrsf14	2.852	0.990	0.991	Tnf receptor superfamily, member 14
Relb	2.769	1.023	0.658	RELB Proto-Oncogene
Ccl4	2.710	1.114	1.672	Chemokine (C-C motif) ligand 4
Tlr13	2.690	0.926	0.727	Toll-like receptor 13
Ccr10	2.589	0.933	1.881	Chemokine (C-C motif) receptor 10
Ccr3	2.403	0.216	0.217	Chemokine (C-C motif) receptor 3
Myc	2.303	1.236	0.776	Myelocytomatosis oncogene
Plp1	2.293	1.287	0.303	Proteolipid protein (myelin) 1
P2ry14	2.237	1.280	2.261	Purinergic receptor P2Y, 14
Sqstm1	2.168	1.280	1.039	Sequestosome 1
Ccl3	2.046	1.141	0.313	Chemokine (C-C motif) ligand 3
Ikbke	1.996	0.961	0.733	Inhibitor of kappaB kinase epsilon

SFN, sulforaphane; GRN, glucoraphanin; NAD(P)H, nicotinamide adenine dinucleotide phosphate; PDGF, platelet-derived growth factor; RELB, v-rel reticuloendotheliosis viral oncogene homolog B.

Table 3. Down-regulated inflammatory genes in the liver of ob/ob mice and normalized by SFN

Gene symbol	ob/ob/normal	SFN/normal	GRN/normal	Gene name
Tspan2	0.415	1.101	0.376	Tetraspanin 2
Fn1	0.508	0.918	0.622	Fibronectin 1
Ticam1	0.533	1.181	0.698	Toll-like receptor adaptor molecule 1
Pik3cd	0.544	0.907	0.352	PI3K catalytic delta polypeptide
Itgb2l	0.568	0.962	1.488	Integrin beta 2-like
Adora2a	0.595	0.988	0.761	Adenosine A2a receptor

SFN, sulforaphane; GRN, glucoraphanin; PI3K, phosphoinositide-3-kinase.

DISCUSSION

This study examined the anti-inflammatory effects of SFN on LPS-stimulated RAW 264.7 macrophage cells. The results showed that SFN increased the DPPH free radical scavenging activity. In addition, SFN suppressed the expression of iNOS, COX-2, and pro-inflammatory cytokines (TNF-α, IL-6, and IL-1β) in LPS-stimulated RAW 264.7 cells. In particular, SFN showed anti-inflammatory effects by normalizing the expression of the genes related to inflammation, including chemokine ligands (Cxcl14, Ccl1, Ccl3, Ccl4, and Ccl17) and chemokine receptors (Cxcr1, Ccr3, and Ccr10), which were perturbed in ob/ob mice liver.

In the present study, SFN showed antioxidant potential through a DPPH assay in a concentration-dependent manner. Previous studies reported that isothiocyanates extracted from broccoli were strongly associated with the DPPH radical scavenging activity [24].

https://doi.org/10.4142/jvs.2020.21.e91

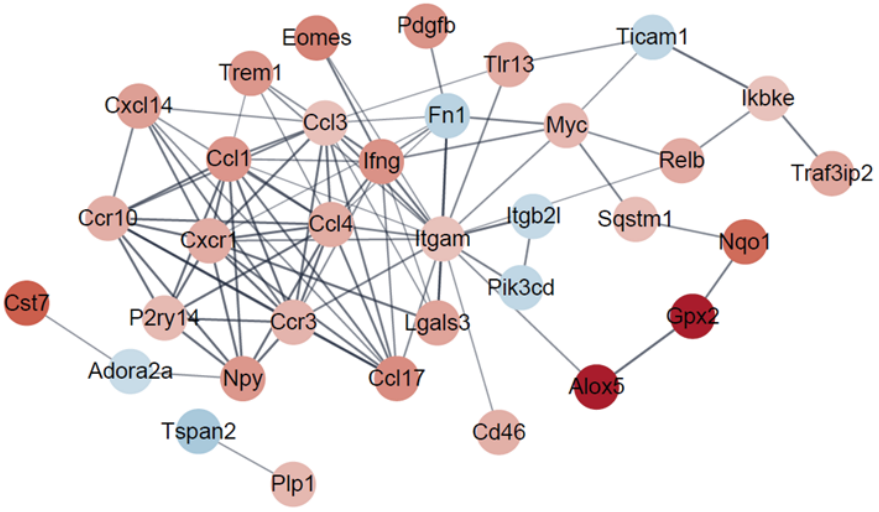

Fig. 7. PPI network of normalized genes related to inflammation in SFN-treated ob/ob mice. Red circles represent up-regulated genes, and blue circles represent the down-regulated genes in the control ob/ob mice.
PPI, protein-protein-interaction; SFN, sulforaphane.

Similarly, in the present study, SFN had potent free radical scavenging activity compared to the GRN. Because oxidative stress induces inflammation [25], the antioxidant activity of SFN might improve the healing procedure of inflammation.

In this study, SFN inhibited the levels of COX-2 and iNOS expression in LPS-stimulated RAW 264.7 cells, with concomitant decreases in NO production. The production of NO by iNOS leads to the activation of macrophages against microorganisms [26]. On the other hand, overexpression of NO, a key biomarker of oxidative stress, causes oxidative damage during the inflammatory process [27]. COX-2 is involved in the production of prostaglandins, which causes an increase in chemotaxis, blood flow, and subsequent dysfunction of tissues during inflammation [28]. The previous study reported that SFN enriched broccoli florets extract suppressed NO production and iNOS expression by inhibiting the NF-κB activity in LPS-stimulated RAW 264.7 cells [29]. In addition, SFN decreased the levels of COX-2 and prostaglandin E_2 in LPS-stimulated RAW 264.7 cells [30]. Consistent with previous findings, the results confirmed that the biological activity of SFN is firmly attributed to the inhibitory effects on COX-2, iNOS, and NO production in LPS-stimulated RAW 264.7 cells. In addition, GRN, without enzymatic conversion to SFN, did not show significant anti-inflammatory effects on LPS-stimulated RAW 264.7 cells compared to SFN.

In the present study, SFN exhibited its anti-inflammatory effects by inhibiting the production of pro-inflammatory cytokines, including TNF-α, IL-6, and IL-1β in LPS-stimulated RAW 264.7 cells. A recent study reported that SFN inhibited the production of TNF-α, IL-6, and IL-1β through activation of the Nrf2/HO-1 pathway and inhibition of the JNK/AP-1/NF-κB pathway in LPS-activated microglia [31]. Therefore the anti-inflammatory effects of SFN might result from the inhibitory effects on the production of pro-inflammatory cytokines in LPS-stimulated RAW 264.7 cells.

In the present study, RNA sequencing analysis was conducted to reveal the molecular mechanism underlying the anti-inflammatory effect of SFN on the obesity-induced inflammation in ob/ob mice. The gene expression results showed that SFN normalized the

https://doi.org/10.4142/jvs.2020.21.e91

expression levels of up-regulated genes related to the inflammation, including Cxcl14, Ccl1, Ccl3, Ccl4, Ccl17, Cxcr1, Ccr3, Ccr10, and Ifng genes in the ob/ob mice liver. Cxcl14 mediated leukocyte migration and differentiation [32]. In addition, Cxcl14 involves the obesity-associated infiltration of macrophages into tissues and hepatic steatosis in obese mice [33]. Ccl1 acts as a chemoattractant for monocytes, immature B cells, and dendritic cells [34]. The inhibition of Ccl1 reduces liver inflammation and fibrosis progression [35]. Ccl3 promotes the recruitment of $CD4^+$ T cells to the liver, and increased Ccl3 expression was observed in the patient with liver injury [36]. Ccl17 shows chemotactic activity for $CD4^+$ T cells and plays a role in trafficking and activation of mature T cells [37]. Furthermore, chemokine receptors (Ccr1, Ccr10, and Ccr3) interact with their specific chemokine ligands, which cause various cell responses, such as chemotaxis [38]. In the liver, IFN-γ activates resident macrophages and stimulates hepatocyte apoptosis by increasing ROS production [39].

Remarkably, in the present study, chemokine ligands (Cxcl14, Ccl1, Ccl3, Ccl4, and Ccl17) and chemokine receptors (Cxcr1, Ccr3, and Ccr10) were identified as hub genes because they formed a "functional cluster" within the PPI network. These results suggest that chemokine proteins might play key roles in the obesity-induced inflammation in ob/ob mice liver. Therefore, the treatment of SFN can normalize liver inflammation by normalizing the up-regulated genes related to chemokines in ob/ob mice liver.

In addition, the current results showed that SFN normalized the down-regulated genes related to inflammation, including Fn1, Itgb21, and Pik3cd in ob/ob mice liver. Fn1 produces soluble plasma fibronectin-1, which is involved mainly in blood clotting, wound healing, and protects against excessive liver fibrosis [40]. Itgb2 encodes CD18, which inhibits the capability of the immune system to fight off infection [41]. Pik3cd regulates the immune cell metabolism through the PI3K-AKT-mTOR signaling pathway [42]. These findings suggest that downregulation of Fn1, Itgb21, and Pikk3cd genes might involve the progress of inflammation by dysregulating immune responses in the ob/ob mice liver.

In conclusion, SFN has a potent anti-inflammatory activity, as demonstrated by its ability to inhibit the NO, COX-2, iNOS, and pro-inflammatory cytokines (TNF-α, IL-6, and IL-1β) in LPS-stimulated RAW 264.7 cells. In particular, gene expression analysis showed that SFN restores the obesity-induced inflammation by normalizing the genes related to chemokine signaling, including chemokine ligands (Cxcl14, Ccl1, Ccl3, Ccl4, and Ccl17) and chemokine receptors (Cxcr1, Ccr3, and Ccr10) in ob/ob mouse livers. Overall, SFN has a potent anti-inflammatory effect by normalizing the expression levels of the genes related to inflammation that had been perturbed in ob/ob mice.

REFERENCES

1. Harrison DG, Guzik TJ, Lob HE, Madhur MS, Marvar PJ, Thabet SR, et al. Inflammation, immunity, and hypertension. Hypertension. 2011;57(2):132-140.
PUBMED | CROSSREF
2. Shapiro H, Lutaty A, Ariel A. Macrophages, meta-inflammation, and immuno-metabolism. Sci World J. 2011;11:2509-2529.
PUBMED | CROSSREF
3. Biswas SK, Lewis CE. NF-κB as a central regulator of macrophage function in tumors. J Leukoc Biol. 2010;88(5):877-884.
PUBMED | CROSSREF

4. Li Q, Verma IM. NF-κB regulation in the immune system. Nat Rev Immunol. 2002;2(10):725-734.
PUBMED | CROSSREF
5. Ye J, McGuinness OP. Inflammation during obesity is not all bad: evidence from animal and human studies. Am J Physiol Endocrinol Metab. 2013;304(5):E466-E477.
PUBMED | CROSSREF
6. Ellulu MS, Patimah I, Khaza'ai H, Rahmat A, Abed Y. Obesity and inflammation: the linking mechanism and the complications. Arch Med Sci. 2017;13(4):851-863.
PUBMED | CROSSREF
7. Hotamisligil GS. Inflammation and metabolic disorders. Nature. 2006;444(7121):860-867.
PUBMED | CROSSREF
8. Sutter AG, Palanisamy AP, Lench JH, Jessmore AP, Chavin KD. Development of steatohepatitis in ob/ob mice is dependent on Toll-like receptor 4. Ann Hepatol. 2015;14(5):735-743.
PUBMED | CROSSREF
9. Perfield JW 2nd, Ortinau LC, Pickering RT, Ruebel ML, Meers GM, Rector RS. Altered hepatic lipid metabolism contributes to nonalcoholic fatty liver disease in leptin-deficient ob/ob mice. J Obes. 2013;2013:296537.
PUBMED | CROSSREF
10. Lauterbach MA, Wunderlich FT. Macrophage function in obesity-induced inflammation and insulin resistance. Pflugers Arch. 2017;469(3-4):385-396.
PUBMED | CROSSREF
11. Santín-Márquez R, Alarcón-Aguilar A, López-Diazguerrero NE, Chondrogianni N, Königsberg M. Sulforaphane - role in aging and neurodegeneration. Geroscience. 2019;41(5):655-670.
PUBMED | CROSSREF
12. Angelino D, Jeffery E. Glucosinolate hydrolysis and bioavailability of resulting isothiocyanates: focus on glucoraphanin. J Funct Foods. 2014;7:67-76.
CROSSREF
13. Xu L, Nagata N, Ota T. Glucoraphanin: a broccoli sprout extract that ameliorates obesity-induced inflammation and insulin resistance. Adipocyte. 2018;7(3):218-225.
PUBMED | CROSSREF
14. Galuppo M, Giacoppo S, De Nicola GR, Iori R, Mazzon E, Bramanti P. RS-Glucoraphanin bioactivated with myrosinase treatment counteracts proinflammatory cascade and apoptosis associated to spinal cord injury in an experimental mouse model. J Neurol Sci. 2013;334(1-2):88-96.
PUBMED | CROSSREF
15. Sotokawauchi A, Ishibashi Y, Matsui T, Yamagishi SI. Aqueous extract of glucoraphanin-rich broccoli sprouts inhibits formation of advanced glycation end products and attenuates inflammatory reactions in endothelial cells. Evid Based Complement Alternat Med. 2018;2018:9823141.
PUBMED | CROSSREF
16. Vo QV, Nam P, Dinh T, Mechler A, Tran T. Anti-inflammatory activity of synthetic and natural glucoraphanin. J Serbian Chem Soc. 2019;84(5):445-453.
CROSSREF
17. Dinkova-Kostova AT, Fahey JW, Kostov RV, Kensler TW. KEAP1 and done? Targeting the NRF2 pathway with sulforaphane. Trends Food Sci Technol. 2017;69(Pt B):257-269.
PUBMED | CROSSREF
18. Li B, Cui W, Liu J, Li R, Liu Q, Xie XH, et al. Sulforaphane ameliorates the development of experimental autoimmune encephalomyelitis by antagonizing oxidative stress and Th17-related inflammation in mice. Exp Neurol. 2013;250:239-249.
PUBMED | CROSSREF
19. Yang G, Lee HE, Lee JY. A pharmacological inhibitor of NLRP3 inflammasome prevents non-alcoholic fatty liver disease in a mouse model induced by high fat diet. Sci Rep. 2016;6(1):1.
PUBMED | CROSSREF
20. Sánchez-Moreno C, Larrauri JA, Saura-Calixto F. A procedure to measure the antiradical efficiency of polyphenols. J Sci Food Agric. 1998;76(2):270-276.
CROSSREF
21. Vuong LD, Nguyen QN, Truong VL. Anti-inflammatory and anti-oxidant effects of combination between sulforaphane and acetaminophen in LPS-stimulated RAW 264.7 macrophage cells. Immunopharmacol Immunotoxicol. 2019;41(3):413-419.
PUBMED | CROSSREF
22. Coleman DL. Obese and diabetes: two mutant genes causing diabetes-obesity syndromes in mice. Diabetologia. 1978;14(3):141-148.
PUBMED | CROSSREF

23. Bai Y, Wang X, Zhao S, Ma C, Cui J, Zheng Y. Sulforaphane protects against cardiovascular disease via Nrf2 activation. Oxid Med Cell Longev. 2015;2015:407580.
PUBMED | CROSSREF

24. Yuan H, Yao S, You Y, Xiao G, You Q. Antioxidant activity of isothiocyanate extracts from broccoli. Chin J Chem Eng. 2010;18(2):312-321.
CROSSREF

25. Salzano S, Checconi P, Hanschmann EM, Lillig CH, Bowler LD, Chan P, et al. Linkage of inflammation and oxidative stress via release of glutathionylated peroxiredoxin-2, which acts as a danger signal. Proc Natl Acad Sci U S A. 2014;111(33):12157-12162.
PUBMED | CROSSREF

26. MacMicking J, Xie QW, Nathan C. Nitric oxide and macrophage function. Annu Rev Immunol. 1997;15(1):323-350.
PUBMED | CROSSREF

27. Tripathi P, Tripathi P, Kashyap L, Singh V. The role of nitric oxide in inflammatory reactions. FEMS Immunol Med Microbiol. 2007;51(3):443-452.
PUBMED | CROSSREF

28. Mitchell JA, Larkin S, Williams TJ. Cyclooxygenase-2: regulation and relevance in inflammation. Biochem Pharmacol. 1995;50(10):1535-1542.
PUBMED | CROSSREF

29. Hwang JH, Lim SB. Bin. Antioxidant and anti-inflammatory activities of Broccoli florets in LPS-stimulated RAW 264.7 Cells. Prev Nutr Food Sci. 2014;19(2):89-97.
PUBMED | CROSSREF

30. Choi WJ, Kim SK, Park HK, Sohn UD, Kim W. Anti-Inflammatory and Anti-Superbacterial Properties of Sulforaphane from Shepherd's Purse. Korean J Physiol Pharmacol. 2014;18(1):33-39.
PUBMED | CROSSREF

31. An YW, Jhang KA, Woo SY, Kang JL, Chong YH. Sulforaphane exerts its anti-inflammatory effect against amyloid-β peptide via STAT-1 dephosphorylation and activation of Nrf2/HO-1 cascade in human THP-1 macrophages. Neurobiol Aging. 2016;38:1-10.
PUBMED | CROSSREF

32. Witte A, Chatterjee M, Lang F, Gawaz M. Platelets as a novel source of pro-inflammatory chemokine CXCL14. Cell Physiol Biochem. 2017;41(4):1684-1696.
PUBMED | CROSSREF

33. Nara N, Nakayama Y, Okamoto S, Tamura H, Kiyono M, Muraoka M, et al. Disruption of CXC motif chemokine ligand-14 in mice ameliorates obesity-induced insulin resistance. J Biol Chem. 2007;282(42):30794-30803.
PUBMED | CROSSREF

34. Roos RS, Loetscher M, Legler DF, Clark-Lewis I, Baggiolini M, Moser B. Identification of CCR8, the receptor for the human CC chemokine I-309. J Biol Chem. 1997;272(28):17251-17254.
PUBMED | CROSSREF

35. Heymann F, Hammerich L, Storch D, Bartneck M, Huss S, Rüsseler V, et al. Hepatic macrophage migration and differentiation critical for liver fibrosis is mediated by the chemokine receptor C-C motif chemokine receptor 8 in mice. Hepatology. 2012;55(3):898-909.
PUBMED | CROSSREF

36. Ajuebor MN, Hogaboam CM, Le T, Proudfoot AE, Swain MG. CCL3/MIP-1α is pro-inflammatory in murine T cell-mediated hepatitis by recruiting CCR1-expressing $CD4^+$ T cells to the liver. Eur J Immunol. 2004;34(10):2907-2918.
PUBMED | CROSSREF

37. Gilet J, Chang Y, Chenivesse C, Legendre B, Vorng H, Duez C, et al. Role of CCL17 in the generation of cutaneous inflammatory reactions in Hu-PBMC-SCID mice grafted with human skin. J Invest Dermatol. 2009;129(4):879-890.
PUBMED | CROSSREF

38. Murdoch C, Finn A. Chemokine receptors and their role in inflammation and infectious diseases. Blood. 2000;95(10):3032-3043.
PUBMED | CROSSREF

39. Crispe IN. The liver as a lymphoid organ. Annu Rev Immunol. 2009;27(1):147-163.
PUBMED | CROSSREF

40. Watanabe Y, Suzuki O, Haruyama T, Akaike T. Interferon-gamma induces reactive oxygen species and endoplasmic reticulum stress at the hepatic apoptosis. J Cell Biochem. 2003;89(2):244-253.
PUBMED | CROSSREF

41. Gjelstrup LC, Boesen T, Kragstrup TW, Jørgensen A, Klein NJ, Thiel S, et al. Shedding of large functionally active CD11/CD18 Integrin complexes from leukocyte membranes during synovial inflammation distinguishes three types of arthritis through differential epitope exposure. J Immunol. 2010;185(7):4154-4168.
PUBMED | CROSSREF

42. Fruman DA, Chiu H, Hopkins BD, Bagrodia S, Cantley LC, Abraham RT. The PI3K pathway in human disease. Cell. 2017;170(4):605-635.
PUBMED | CROSSREF